Analysis of the impact of wildland-urban-interface fires on LPG domestic tanks

Giordano Emrys Scarponi[a], Elsa Pastor[b], Eulàlia Planas[b], Valerio Cozzani[a,*]

[a] LISES – Department of Civil, Chemical, Environmental and Materials Engineering, Alma Mater Studiorum – University of Bologna, via Terracini 28, 40131 Bologna, Italy
[b] Department of Chemical Engineering, Centre for Technological Risk Studies, Universitat Politècnica de Catalunya·BarcelonaTech, Eduard Maristany 10-14, E-08019 Barcelona, Catalonia, Spain

ABSTRACT

Managing Wildland-Urban-Interface (WUI) fires is a challenging task due to the inherent complexity of the WUI environment. To ensure the success of strategies for the protection of population and structures, safety measures have to be implemented at different scales (landscape, community and homeowner). The present study is focused on the homeowner scale and deals with the threat related to the presence of LPG domestic tanks in a WUI fire scenario. Recent accidents have demonstrated that the risk associated with this type of installation is real, but often disregarded by residents. A methodology was developed, providing a set of indicators that may easily be compared with risk acceptance criteria, assessing whether the integrity of an LPG tank exposed to WUI fire scenarios is compromised or not. The methodology is applicable to a vast range of situations and at a different level of detail according to available data. A number of case studies were carried out, showing that WUI fire scenarios impacting on domestic LPG tanks complying with regulations currently adopted in several Mediterranean countries cannot be deemed safe. The methodology proposed represents an advanced tool to assist on safety distances sizing to be prescribed by standards, driving regulators towards better-informed decision-making.

1. Introduction

Forest fires affecting urban and rural communities represent an increasing problem throughout the world. They pose tremendous management challenges in terms of civil protection and fire mitigation (Manzello et al., 2018). These emergencies often exceed fire-fighters capacities due to their multi-risk nature: they usually involve wildfire suppression, structures protection and communities' evacuation, and they can even trigger Natech events when interfacing industrial infrastructure (Cozzani et al., 2014; Khakzad, 2019; Khakzad et al., 2018; Krausmann et al., 2011; Naderpour et al., 2019).

The WUI (wildland-urban interface) fire problem is inherently complex, as it is characterized by the interaction of multiple phenomena of diverse nature occurring at different observation scales: the macroscale or landscape scale, the mesoscale or settlement scale and the microscale or home/plot scale (Elsa Pastor et al., 2019). It is at the microscale where the specific events that jeopardize residents and assets can be observed and where prevention actions at home-owner level must be undertaken. The WUI microscale is quite often characterized by the presence of all sorts of combustible elements around structures

(ground fuels, ornamental vegetation, stored material, etc.) whose hazard is poorly characterized and thus remarkably disregarded by residents (Elsa Pastor et al., 2019).

The hazard associated with domestic LPG (liquefied petroleum gas) storage tanks, used as energy source for heating, hot water production or cooking in WUI developments has to be highlighted in this framework. This type of infrastructure may be seriously threatened by a fire, particularly in those cases where negligence or regulatory gaps allow a very close exposure of these tanks to flames coming from nearby fuels. In these situations, the tank will heat up and the pressure will start increasing. If the tank pressure reaches the Pressure Relief Valve (PRV) set point, this will open, releasing LPG that will immediately ignite forming a jet fire. The jet fire will hence worsen the heat load to the tank and the surroundings. If no measure is taken in order to cool down the tank and/or extinguish the fire, the tank may fail, leading to a loss of containment. Depending on the type of failure, intense jet fires from shell cracks, BLEVEs (Boiling liquid Expanding Vapor Explosions) and fireballs may follow (Abbasi and Abbasi, 2007; Birk and Cunningham, 1994; Leslie and Birk, 1991; Mcdevitt, 1990; Moodie et al., 1985). Furthermore, fragments resulting from the destruction of the tank shell

---

Nomenclature

A	Fire surface area (m^2)
A_W	Constant in the wind profile equation (–)
d_{w0}	Height above the ground at which zero wind speed is achieved (m)
E	Fire emissive power (W/m^2)
f	View factor (–)
$f_{F \to P}$	View factor between the fire and point P on the tank surface (–)
h_g	External convective heat transfer coefficient (W/m^2 K)
HRR	Heat release rate (W)
I	Incident radiation (W/m^2)
I_P	Incident radiation on point P on the tank surface (W/m^2)
Na	Nusselt number (–)
$PRVI$	Pressure Relief Valve Index (–)
p_{max}	Maximum pressure reached in the tank (bar)
p_{PRV}	Pressure relief valve set point (bar)
$\dot{q}''$	Heat flux (kW/m^2)
Ra	Rayleigh number (–)
$S_{a,max}$	maximum surface area where the temperature is higher than 400 °C (m^2)
S_c	critical surface area (0.48 m^2)
t	Time (s)
$T_{BB,eq}$	Equivalent black body temperature (K)
T_g	Temperature of the gas in contact with the outer tank wall (K)
T_w	Wall temperature (K)
T_∞	Ambient temperature (K)
U	Wind speed (m/s)
u_{10}	Wind speed at 10 m above the ground (m/s)
V	Tank valume (m^3)
WSI	Weakened Surface Index (–)
x	Generic coordinate (m)
χ_R	Radiative fraction (–)
Z	Elevation from the ground
z_0	Ground roughness (m)
σ	Stefan-Boltzman constant (8.57·10^{-8} W/(m^2 K^4)
ε_w	Wall emissivity (–)
ε_w	Fire emissivity (–)
Γ	Air transmissivity (–)

can be projected to the surrounding, potentially worsening the consequences of the explosion (Tugnoli et al., 2013).

In recent WUI fire events (e.g. Benitatxell, Spain, 2016; Madeira, Portugal, 2016; Calabassas, California, 2016; Mati, Greece, 2018) these type of infrastructures were dangerously affected (Fig. 1). The lack of an effective safety distance between the LPG tank and the surrounding fuels caused the opening of the safety relief valves and intense jet fires. Although explosions did not occur, the magnitude of the consequences in case of a BLEVE-Fireball event could have been severe, given the high population and assets density that usually characterize WUI areas. Being able to assess whether a given fire scenario represents or not a threat for LPG tanks integrity is therefore critical to ensure safety of this type of installations.

Looking at the problem under the perspective of a bow-tie analysis (Delvosalle et al., 2006), the event "vessel failure" can be considered as the critical event in the center of the bow-tie diagram. As suggested by Reniers et al. (2018), the natural event (the WUI fire in this case) is on the fault tree side, while the consequences of the vessel failure (BLEVE, fireball, missiles projection) are on the right side (event tree).

Models for the estimation of the consequences generated by the final events, such as overpressure and thermal radiation, are well established in literature (Uijt de Haag and Ale, 1999). Even if these models were mainly developed considering accident scenarios typical of the process industry, they are independent from the fire conditions leading to the tank failure and can therefore be applied also in the case of LPG tanks exposed to wildfires and WUI fires.

On the other hand, the analysis of the left wing of the bow-tie is specific and, to be effective, requires a dedicated approach. This must encompass the detailed characterization of the fire scenario, the description of the heat transfer from the fire to the tank and, finally, the assessment of the tank vulnerability. As discussed in the following, the first of these three points (the characterization of the fire scenario) is particularly critical. However, most of the wildfire spread models available cannot cope with the complexity of wildfires behaviour when they approach the WUI (Rehm and Mell, 2009).

This paper presents a comprehensive study of the problem of LPG domestic tanks exposure to WUI fires, addressing mostly the left wing of the bow tie-diagram. First, an analysis of the existent regulations in European countries prone to wildfires and fires at WUI is carried out, with the aim of detecting gaps, deficiencies and inconsistencies between regulations. The focus is mainly on the definition of separation and safety distances between the tank and the flammable materials and/or vegetation that represent a measure to prevent tank failure. Current approaches to fire characterization at the WUI and vulnerability assessment of LPG tanks exposed to fire were reviewed. A methodology was developed to support the assessment of LPG tanks integrity in WUI fire scenarios. The methodology is based on a three step approach addressing fire source characterization at different levels

Fig. 1. (a) Calabassas fire (California, 2016 – credit KABC-TV). A propane jet fire can be observed at the center of the image (inside the yellow dotted ellipse). Flames from ornamental fuels are close to the tank. LPG infrastructure was inside a kindergarten; (b) Domestic LPG tank in Benitatxell (Spain, 2016 - credit D. Caballero) damaged by a jet fire from the PRV. The tank was surrounded by an ornamental hedgerow that ignited by spotting. (For interpretation of the references to colour in this figure legend, the reader is referred to the web version of this article.)

of detail and on the assessment of LPG tank vulnerability based on a CFD (Computational Fluid Dynamics) model.

2. Regulatory framework at European level

Worldwide the use and installation of domestic LPG tanks is not harmonized. In the European Union, different regulations are issued by each Member State (MS). Thus, prescription specifying, among others safety distances from the LPG supply unit to vulnerable elements, storage of flammable materials and sources of ignitions, may be extremely variable. A detailed and comprehensive analysis of all regulations is out of the scope of the present study. In the following, regulations from France (JORF, 1979), Greece (ΦEK, 1993), Italy (GUDRI, 2004) Portugal (DRE, 2002), Spain (AENOR, 2008) and UK (HSE, 2016) will be considered for the sake of comparison and to analyze the specific case-studies.

Fig. 2 shows a comparison of minimum safety distances from domestic above-ground LPG tanks according to the legislation of the European countries listed above. In general, it can be noted how prescriptions are not harmonized. Italy has the most conservative requirements, whereas Spain has the less restrictive ones. The Spanish regulation, for instance, indicates that for tanks with volume within 1 and 5 m^3 in volume, safety distances should be of 2 m. This distance can be reduced by a 50% for smaller tanks. The Italian legislations prescribes a safety distance that is more than twice of that required in Spain for the same tank volumes. Thus, strong discrepancies are present in the standards, even within countries in the same geographical area and exposed to similar hazards. This alone should rise concern.

Another important issue that is worth to remark is that not all the standards in the different countries listed in Fig. 2 explicitly regulate the possible presence of vegetation in the proximity of the tank. The Greek regulation clearly states that "*the floor of the storage area must be kept clean and free of dry grass, grass and foreign objects*". Similarly, the HSE (UK) recommends that there should be no trees or shrubs within the safety distance reported in the standard. The Italian regulation requires that no vegetation is present in an area of 5 m around the tank. On the other hand, the Portuguese regulation has a more general statement, not allowing the presence of flammable products within the safety distance reported in Fig. 2. The French regulations simply mention that no storage of flammable material can be present in the area defined by safety distance. Clearly enough, such statement does not cover the case of ornamental vegetation commonly placed in WUI microscale and that might be ignited in case of wildfires. The Spanish regulation does not address the issue of the possible presence of fuels in the proximity of LPG tanks.

Indeed, there are countries in which the potential hazard produced by the presence of vegetation in the proximity of LPG tanks is not properly considered. As shown in Fig. 1, this regulatory gap may produce dangerous situations in case of WUI fires. Furthermore, even in the countries with a standard explicitly addressing the issue, situations such as those depicted in Fig. 1 demonstrate that current prescriptions might be not sufficient to avoid escalation events involving domestic LPG tanks in the case of severe wildfires.

In the framework of such jeopardized scenario, the need clearly emerges to support regulators towards better-informed decision-making in the determination of safety distances.

3. Current approaches to fire characterization in WUIs and vulnerability assessment of LPG tanks exposed to fire

Addressing the problem of the assessment of LPG tanks vulnerability in WUIs requires to focus the attention on two aspects. The first is the characterization of the fire behavior in such a complex environment. The second concerns the analysis of the response of LPG tanks to fire exposure in the specific conditions present in WUIs.

3.1. Fire source characterization at the WUI

Wildfires spread is usually described as an advancing fire front featuring specific intensity, rate of spread, and flame height, which are influenced by the landscape characteristics, the weather conditions and the fuel properties (Rehm and Mell, 2009). This description is at the base of the most common wildfire models, such as FARSITE (Finney, 1994) and FlamMap (Finney, 2006), which are designed to predict the wildfire spread for long periods of time (hours to days) and over large areas (in the order of several square kilometers), where the fuel type distribution can be considered quite uniform (an extensive review of wildfire simulators is presented by Sullivan (2009). However, as pointed out by Murphy et al. (2007), observations show that wildfire behavior may change considerably when the fire front approaches the WUI. Here, local variations in the type and spatial distribution of fuel play an important role in the way the fire spreads and affects structures (Rehm and Mell, 2009).

Affectation of structures due to the presence of fire at the WUI is a complex and multistep process. Considering a single lot (i.e. a house together with the set of objects/ornamental vegetation in its proximity), the sequence of events characterizing the interaction with a wildfire can be divided in four phases: Pre-impact, Impact, Fire transfer and Post-fontal combustion. The Pre-impact is the phase in which a nearby fire is approaching the settlement, but has not reached the house yet. As the fire front gets closer, the probability that that smoke and flying embers transported by wind reach the lot, the garden elements and the house increases. These firebrands may set fire in vegetation, ornamental plants and several other materials and objects present in the garden near the house or the house itself. In the Impact phase, the fire front is facing the house at such a distance that thermal radiation (and sometimes flame impingement) have a direct effect on the house and the surrounding items, the ignition of which is quite likely. If this happens, the fire propagates through the elements in the lot (Fire transfer phase), with the possibility of triggering more and more fires. Finally, in the Post-frontal combustion phase, all the objects, materials and house parts that ignited in any of the previous phases continue burning with or without flames for longer periods, possibly causing further escalation.

As pointed out by Mell et al. (2009), large scale wildfire spread models cannot deal with the complexity of such process. For this reason, they cannot be effectively applied to assess the fire risk at the WUI. They suggest that the solution may be represented by the development of validated physics-based numerical models such as WFDS.[1]

According to Rehm and Mell (2009), one of the main issues is represented by the large spectrum of spatial and time scales associated with wildfires at the WUI. An interesting approach to address the multiscale nature of the problem of assessing the wildfire impact on a specific target was proposed by and Khakzad (2019), where a strategy to link large scale wildfire simulator results with vulnerability models working at a much smaller scale is presented. Here, the fire spread is simulated using an approach that integrates a dynamic Bayesian network with data provided by the Canadian Forest Fire Behavior System, whereas the impact on the target (in this case an atmospheric tank placed in an oil terminal) is estimated using the expression for the calculation of the time to failure proposed by Landucci et al. (2009). Such equation was derived using an integral model for the fire response of pressure vessels and requires as input the heat load received from the vessel to the fire. The link between the wildfire spread model and the vulnerability model is represented by a solid flame model (see Section 4.1 for more details) that takes as input the fire intensity provided by the wildfire spread model and provides as output the heat load to be used in the equation for the estimation of the time to failure.

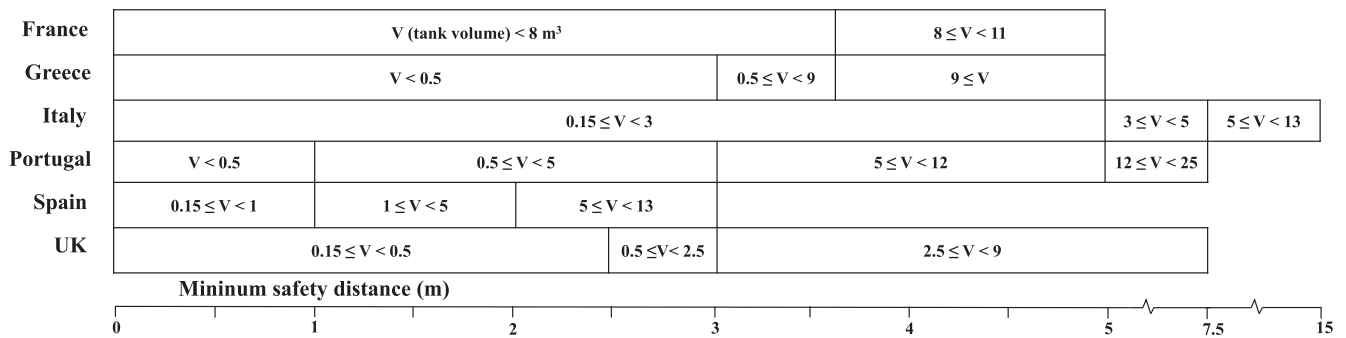Undoubtably, the work of Khakzad (2019) introduces an important

---

[1] https://www.fs.fed.us/pnw/fera/research/wfds/.

Country						
France	V (tank volume) < 8 m³				8 ≤ V < 11	
Greece	V < 0.5			0.5 ≤ V < 9	9 ≤ V	
Italy	0.15 ≤ V < 3					3 ≤ V < 5 / 5 ≤ V < 13
Portugal	V < 0.5	0.5 ≤ V < 5		5 ≤ V < 12	12 ≤ V < 25	
Spain	0.15 ≤ V < 1	1 ≤ V < 5	5 ≤ V < 13			
UK	0.15 ≤ V < 0.5		0.5 ≤V< 2.5	2.5 ≤ V < 9		

Minimum safety distance (m)

0   1   2   3   4   5   7.5   15

Fig. 2. Minimum safety distances as a function of tank volume V (in m³) for different European countries.

improvement the field of the assessment of wildfire risk on industrial plants. However, the proposed approach is not specifically developed to capture the features of WUI fire scenarios.

3.2. LPG tank vulnerability

The response of LPG vessels to fire exposure was investigated since the sixties (Bray, 1964). Several fire test campaigns have been carried out by different research groups and institutions (most of which are summarized in the literature reviews presented by Moodie (1988a,b) and Birk (2006)), which allowed increasing the understanding of the physical phenomena involved in these scenarios (e.g. Aydemir et al., 1988; Sumathipala et al., 1992; Birk and Cunningham, 1996).

In parallel to experimental studies, more and more complex models were developed over the years, aimed at reproducing the phenomena occurring inside a vessel under fire exposure, and predicting pressurization rate, temperature distributions and time to failure. Early approaches are based on strong simplifying assumptions (Aydemir et al., 1988; Beynon et al., 1988; Birk, 1988, 1983; Germany et al., 1990; Gong et al., 2004; Graves, 1973; Johnson, 1998b, 1998a; Venart, 2000; Yu et al., 1992): the tank is divided in one or more zones (or nodes), for which integral mass and energy balances are solved. Such models rely on empirical expressions with a limited range of applications. Furthermore, they neglect key phenomena such as thermal stratification and boiling. More recently, approaches based on CFD codes were proposed (Bi et al., 2011; D'Aulisa et al., 2014; Hadjisophocleous et al., 1990; Scarponi et al., 2019, 2018a; Yoon and Birk, 2004).

Despite such advancements, the vast majority of the studies addressed the effects of hydrocarbon pool and jet fires (i.e. scenarios that are likely to occur in an industrial environment). So far, very little attention was dedicated to the analysis of pressure tanks exposed to fire in WUI scenarios. Heymes and co-workers (2013c, 2013b) recently carried

out a study specifically addressing such framework, performing a set of fire tests on a 2.3 m³ LPG tank exposed to a distant source of radiation, mimicking the effect of a forest fire. They considered a crown fire scenario with a 100 m wide by 40 m high fire front and average (and constant) emissive power of 90 kW/m², affecting a tank positioned at 50 m from the fire. They also provided a method to estimate safety distances (Heymes et al., 2013a) based on the guideline provided in the API 2501 (American Petroleum Institute, 2001). Few years later, Scarponi et al. (2018b) proposed a 2D CFD modelling setup able to reproduce with good accuracy the experimental results obtained by Heymes and co-workers (2013c, 2013b).

Although the above mentioned publications represent pioneering works in the field, a comprehensive analysis of the problems related to fire affecting pressure vessels at the WUI is still missing.

4. Methodology proposed for the assessment of LPG tank vulnerability at the WUI

In the light of the above discussion on the assessment of the effect of wildfires on specific targets at the WUI, the methodology presented here can be considered as the connection between large scale wildfire spread simulations and the meso and microscale approach needed to correctly model WUI fires. The methodology proposed addresses the representation of WUI fire and the tank integrity assessment. This is done following the three steps represented in Fig. 3: the characterization of the fire source (e.g. flame shape, emissive power, transient behavior), the simulation of the tank response (e.g. pressurization rate, steel and lading temperatures) and the tank integrity assessment, which addresses the threat posed by the scenario.
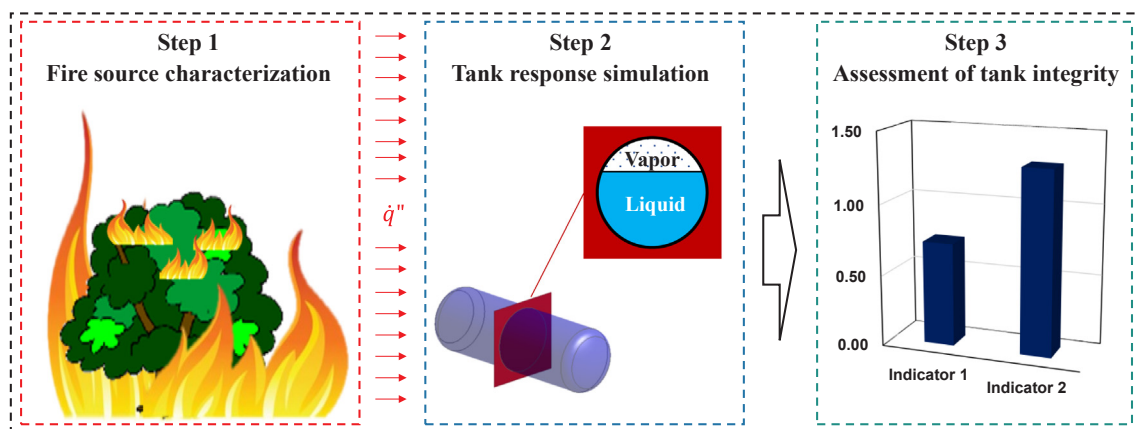

Fig. 3. Schematization of the problem and of the methodological approach ($\dot{q}''$ is heat flux through the external surface of the tank). Indicators are defined in Section 4.3.

4.1. Step 1 – Fire source characterization

The aim of the first step (the red block in Fig. 3) is to characterize the fire scenario, providing the inputs required for the analysis of the tank response. Thus, the heat load coming from the fire needs to be defined. This is usually carried out defining the heat flux ($\dot{q}''$) induced by a fire on a LPG tank (as well as for any generic target, at time t and at point $\vec{x}$ on the target external surface) as the sum of radiative and convective contributions as expressed by Eq. (1):

$$\dot{q}''(\vec{x}, t)$$
$$= \sigma \varepsilon_w (T_{BB,eq}(\vec{x}, t)^4 - T_w(\vec{x}, t)^4) + h_g(\vec{x}, t)(T_g(\vec{x}, t) - T_w(\vec{x}, t)) \tag{1}$$

where σ is the Stefan-Boltzman constant, ε_w is the emissivity of the wall, T_w is the wall temperature and $T_{BB,eq}$ is the equivalent black body temperature (representative of the incident radiation hitting the tank surface):

$$T_{BB,eq}(\vec{x}, t) = \sqrt[4]{\frac{I(\vec{x}, t)}{\sigma}} \tag{2}$$

The values of the incident radiation I (representing the radiative contribution of both the fire and the ambient), the temperature of the gases T_g (air, flame, smoke) in contact with the tank surface and the convective heat transfer coefficient h_g need to be specified according to the fire scenario characteristics. The definition of such parameters is the particular objective of the first step of the methodology (the red block in Fig. 3). It is worth mentioning that, in cases where no direct impingement of the flames on the tank occurs, the convective term in Eq. (1) can be neglected. In these cases, this term would actually be negative (i.e. involving convective cooling of the tank surface), hence neglecting it results in a conservative approach from the safety standpoint. Therefore, in scenarios with no flame impingement, spatial and temporal distribution of the incident radiation is the only required input.

As pointed out by Mell et al. (2009), in order to effectively carry out a fire risk assessment at the WUI, it is crucial to be able to properly reproduce the fire behavior. This entails the use of tools that are able to accurately capture fire transient characteristics at small spatial and time scales, such as the flame geometry end emissive power.

In the present methodology, three different approaches (options) are proposed to carry out the fire characterization step. The level of detail they provide in terms of description of the fire behavior at the micro and meso scales increases going from the first one to the last one. The selection of the approach to be used depends on available data, accuracy required and organizational factors such as time, costs and computational resources.

Table 1 presents an overview of the possible options for the characterization of the fire scenario. The table also specifies the main inputs

and the tools required to apply each approach.

Option 1 represents the case in which the analyst already knows the heat load to be applied to the storage tank (e.g. when this comes from regulations, standards, prescriptions or experience). In this case it is possible to directly proceed with the definition of I, h_g and T_g (see Eqs. (1) and (2)).

Option 2 is based on the solid flame model concept (Eisenberg et al., 1975): the flame is considered as a solid body having defined shape and dimensions, with an emissive power E. Thus, the incident radiation I to remote points (e.g. the tank surface) is obtained using Eq. (3), where Γ is the air transmissivity (which is a function of the humidity and the concentration of the carbon dioxide in the atmosphere and can be calculated using empirical correlations) and f is the view factor between the remote point and the solid body representing the flame. Details about the calculation of the view factor under the assumption of uniform radiosity and that both the flame and the object surface emit and reflect diffusely can be found in the literature (Beatty, 2004; Eckert, 2004; Heymes et al., 2013c; Modest, 2003; Scarponi et al., 2018b).

$$I = \Gamma f E \tag{3}$$

$$E = \varepsilon_F \sigma T_F^4 \tag{4}$$

$$E = \frac{\chi_R \text{HRR}}{A} \tag{5}$$

An example of application of Option 2 is reported by Scarponi and Heymes (2018), who considered the situation of a LPG tank exposed to the front of a wildfire. In the study, the fire emissive power and the flame shape were defined according to real scale experimental measurements and only a view factor calculation was needed to obtain I (a unitary value of air transmissivity was assumed).

When fire emissive power and flame shape are not readily available, they should be derived. Two alternative routes are possible for the calculation of the fire emissive power: in the case of flames that can be approximated as a radiant grey body (i.e. for which the radiant intensity is independent of the wave length), Stefan-Boltzamann's law (Eq. (4)) can be used, where ε_F and T_F are the flame emissivity and temperature respectively. Alternatively, when ε_F and/or T_F are unknown, Eq. (5) is considered. The latter is based on the Heat Release Rate (HRR) concept. According to the definition reported in the SFPE handbook (Hurley et al., 2002) the HRR is the rate at which the combustion reactions produce heat and is considered as *"the single most important variable in fire hazard"* (Babrauskas and Peacock, 1992). HRR curves are available from many sources in literature. For instance, the SFPE Handbook (Hurley et al., 2002) reports HRR curves for a series of common residential fuels (e.g. pallets, trash containers, bushes, etc.). Only a fraction χ_r (radiative fraction) of the heat produced by the combustion reactions is released in the form of radiation. Values of χ_r are reported in literature for several common fuels (Hurley et al., 2002).

Table 1
Different strategies to characterize the fire sources considered.

Option	Main inputs	Required tools
(1) Direct definition	- Expert judgment or prescriptions	- None
(2) Solid flame model	- Scenario geometry	- Tool for the calculation of view factors
	- Fire emissive power (as a function of time) or fire Heat Release Rate curve (and radiative fraction)	
	- Fire shape	
(3) Fire simulation	*3.1 – Fire prescription*	- Fire simulation software (e.g. FDS)
	- Scenario geometry	
	- Fire HRR curve	
	- Ambient conditions (temperature, humidity and wind)	
	3.2 – Fire prediction	
	Scenario geometry	
	Solid fuel composition, density, heat capacity and thermal conductivity	
	Solid fuel particle size distribution and moisture content (for vegetation)	
	Solid fuel pyrolysis curve	
	Ambient conditions (temperature, humidity and wind)	

The last parameter needed for the evaluation of Eq. (5) is the surface area (A) of the solid representing the flame, which depends on the shape of the fire. This must be estimated using empirical formulas correlating it to the HRR, as those proposed by Anderson et al. (2006). The fire shape is also needed for the calculation of the view factor in Eq. (3).

By this approach, a complete characterization of the incident radiation I is obtained. As for the temperature of the gas in contact with the tank wall and the related convective heat transfer coefficient (T_g and h_g in Eq. (1)), it must be pointed out that the solid flame model is only valid for a distant fire source. This means that scenarios involving flame impingement cannot be analyzed using this method and that the use of Option 2 is limited to fire scenarios in which the flame is not in contact with the wall of the tank. In such cases, the gas temperature T_g can be considered as the ambient temperature. The convective heat transfer coefficient h_g can be estimated through empirical correlations for the calculation of the natural convection heat transfer coefficient around a horizontal cylinder, as the one reported by Martynenko and Khramtsov (2005):

$$Nu = 0.13Ra^{1/3} \qquad (6)$$

where Ra is the Rayleigh number and Nu is the Nusselt number ($Nu = \frac{h_g D}{k_{air}}$; where D is the tank diameter and k_{air} is the thermal conductivity of the air). Typical values for h_g in cases like the ones of interest here range between 1 and 10 W/(m^2 K).

The last option to carry out the fire source characterization step is the use of a fire simulation software (Option 3), in which the scenario under analysis is reproduced and spatial and temporal distributions of I, h_g and T_g on the surface of the target object (in this case the LPG tank) are obtained. In the present methodology, the Fire Dynamic Simulator (FDS) by the National Institute of Standards and Technology (NIST) of the Unites States Department of Commerce is considered as the reference tool to carry out the simulations. The key point when considering Option 3 is how the fire is simulated. Two different options were defined to carry out the simulation: Option *3.1 – Fire Prescription*, and Option *3.2 - Fire Prediction*. The first option consists of simulating a burning element as a solid shape with an assigned HRR curve on its surface. The software models the fire as the ejection of a gaseous fuel from the surface that ignites, generating the flame. This procedure is similar to that of Option 2, with the important difference that I, h_g and T_g on the target are obtained by the fire simulator solving the transport equations for mass, momentum and energy (including radiation transport) through the problem domain.

Option 3.2 represents the most advanced approach to the simulation of a fire scenario, fully exploiting the capabilities of the fire simulation software in the modelling of the combustion of solid fuels. All the steps characterizing the combustion process of a solid fuel are considered (although applying some simplifying assumptions according to data availability and required level of detail): the heat-up phase, the pyrolysis process leading to the production of gaseous fuels and the final burning process (a comprehensive description of such processes can be found in Hurley et al. (2002). In other words, the heat released from the fuel surface is not prescribed (as it is in Option 3.1 using a HRR curve), but rather predicted using the potentialities of the fire simulator.

Due to the ability of capturing local fire characteristics with a high degree of detail, it is advisable, when data are available, to carry out the fire source characterization by Option 3. This approach also allows simulating scenarios in which fire impingement takes place.

4.2. Step 2 – Tank response analysis

The previous step allows obtaining the spatial and time varying maps of I, h_g and T_g on the tank surface. The setting of these parameters represents the boundary condition for the simulation of the tank response when affected by a fire. In the methodology presented here, this is carried out by a CFD analysis. The ANSYS® Fluent® 18.2.0 code was used, applying the CFD modelling setup proposed by Scarponi et al. (2019). The tank (both the steel wall and the lading) is discretized in a computational grid and governing equations for mass, momentum, energy and turbulent quantities are solved throughout the computational domain. According to the computational resources and the geometrical characteristics of the scenario to be analyzed (i.e. if I, h_g and T_g may be considered constant along the axial direction of the tank), a 2D or a 3D approach can be applied. Further details on the possible approaches to be applied in this step are reported in literature (Scarponi et al., 2019, 2018a; Tugnoli et al., 2019).

The application of the CFD procedure provides a large amount of data describing the thermo-fluid dynamic response of the vessel to fire exposure. In particular, it is possible to obtain pressurization curves, wall temperature profiles, temperature distribution in the liquid and vapor phases and evolution of the velocity field.

4.3. Step 3 – Assessment of tank integrity

In the last step of the methodology, the results of the CFD simulations are analyzed with the aim of understanding whether the fire scenarios under consideration may compromise tank integrity.

According to the API 2510 (American Petroleum Institute, 2001), the integrity of an LPG tank exposed to fire is not compromised as long as: i) the tank is equipped with a properly designed PRV (i.e. the PRV prevents the vessel pressure from rising more than 21% above the design pressure) and ii) the incident radiation is below 22 kW/m^2. This is a very useful indication and may even avoid the necessity of carrying out the second step of the methodology. In fact, the value of the incident radiation is already available after the fire characterization (Step 1).

However, assuming the threshold value suggested by API 2510 (22 kW/m^2) would often be over-conservative. Furthermore, the radiation threshold value provided was derived considering a distant fire source and is not valid in case of flame impingement.

Therefore, it is important to have alternatives to establish whether the tank integrity may be compromised by the fire scenario defined in step 1. It is well known that tank failure mainly occurs due to high wall temperatures. In fact, steel strength degradation at high temperatures may produce a failure even when the vessel pressure is within design limits (Manu et al., 2009). Assessing whether the tank would fail under specific fire conditions would require a detailed stress analysis based on full geometrical and mechanical details of the tank, which is out of the scope of the present study. A simplified approach to assess the possible mechanical weakening of the tank structure induced by the fire was presented by Scarponi et al. (2017). The authors introduced a "Strength Index" defined as the ratio between the surface area of the tank wall

Table 2
Indicators for the assessment acceptability of the LPG tank response to fire.

Indicator	Definition	Notes
WSI: Weakened Surface Index	$WSI = \frac{S_{a,max}}{S_c}$	$S_{a,max}$: maximum (over simulation time) surface area where the temperature is higher than 400 °C S_c: critical surface area (0.48 m^2)
PRVI: Pressure Relief Valve Index	$PRVI = \frac{p_{max}}{p_{PRV}}$	p_{max}: maximum pressure reached in the tank p_{PRV}: PRV set point

suffering mechanical weakening, identified as the surface area of the tank outer wall within which the temperature is higher than 400 °C, and the total surface area of the tank. The temperature of 400 °C was selected since above this value the yield strength of plain carbon steel is decreased by 70% with respect to ambient temperature (25 °C) conditions (Birk, 1995). In the present study, a "Weakened Surface Index" (WSI) is introduced as defined in Table 2. This is based on the "Strength Index" with two modifications. The numerator of the WSI is defined as the maximum extension of the tank outer wall surface area in which the temperature exceeds 400 °C over the simulation time ($S_{a,max}$). This modification is required since the "Strength Index" refers to steady state conditions, which is not the case of the scenarios of interest in the present study. The second modification is the replacement of total tank wall surface area at the denominator with the critical surface area, S_c (see Table 2). This parameter was derived from the work by Birk (2005), who studied the effect of defective thermal protection coating on LPG tanks exposed to fire. Birk (2005) suggests that a rectangular defect larger than 1.2 × 0.4 m (resulting in a surface area of 0.48 m²) may cause a tank rupture in case of fire exposure. Here, this concept is extended considering that, if a fire generates a hot zone on the tank wall larger than S_c, the tank integrity is no longer ensured. Values of WSI higher than 1 indicate that the fire scenario under analysis represents a threat for the tank integrity.

An additional critical point is represented by the PRV opening. In fact, although such event represents a safety measure to prevent the tank rupture, the jet fire resulting from the ignition of the fluid released by the valve increases the heat load to the tank and may contribute to worsen the consequences of the fire. Therefore, it is reasonable to assume that scenarios in which the tank pressure reaches the PRV set point are not desirable. For this reason, the Pressure Relief Valve Index (PRVI) is introduced. This is the ratio between the maximum pressure reached during the tank response simulation and the PRV set point pressure (see Table 2).

From the definitions presented above, fire scenarios resulting in values WSI and PRVI higher than 1 have the potential to compromise tank integrity and/or to results in an escalation of consequences. However, WSI and PRVI are only lumped indexes representative of potentially hazardous conditions. WSI depends on the value of S_c, that was derived bay extrapolation of experimental observations and shell be considered as an indicative critical value rather than an exact threshold. On the other hand, the PRVI is based on the value of the PRV set point. However, due to the high temperature reached under fire exposure, the spring in the PRV may experience softening (Heymes et al., 2013b), resulting in an actual opening pressure lower than the design one. In the following, considering both these factors of uncertainty, a safety coefficient of 0.9 was applied to identify scenarios not having the potential to compromise the integrity of LPG installations.

5. Case studies

A set of case studies is presented here with the aim of demonstrating the application of the methodology proposed in the previous section. Two different fire scenarios were analyzed. In the first (that will be referred as "Scenario 1" in the following), a tank is exposed to a fire from a neighboring burning fuel bed of *Pinus halepensis* slash. In the second scenario ("Scenario 2"), the tank is exposed to a burning hedgerow of Douglas fir trees. More details on the two fire scenarios are given below.

In both cases, the reference target is a 1 m³ LPG tank (diameter = 1000 mm, length = 1470 mm, wall thickness = 6 mm, with semi-elliptical ends) distant 3 m from the fire, which is in compliance with the safety distances prescribed in Portugal, Spain and UK (see Fig. 2)

The aim of the analysis of Scenario 1 is to provide a detailed description of how each of the steps in Fig. 3 is carried out. In Scenario 2, the focus is on the application of Option 3.1 and 3.2 proposed to carry out the fire source characterization (the first step in Fig. 3). As discussed in the following, none of the scenarios analyzed considers fire impingement. It is important to remark that this is only due to the specific characteristics of the selected scenarios and should not be intended as a limitation of the proposed methodology. Actually, impingement or engulfment scenarios are not the more representative scenarios expected for WUI fires involving LPG tanks, and fire impingement on LPG tanks is extensively addressed in several literature studies (e.g. see Moodie (1988), Leslie and Birk, (1991) and papers cited therein).

5.1. Scenario 1

Scenario 1 involves quite severe fire conditions, the characteristics of which were derived from fire experiment monitoring (E Pastor et al., 2019). In this fire test, a 13 m by 6 m fuel bed of *Pinus halepensis* slash (the average height of which was approximatively 1.5 m) was ignited with the aim of studying a fire front close to a vulnerable target. This scenario represents cases in which the neighboring plot to the one having the LPG tank is abandoned and accumulated unmanaged fuel having the potential to burn. Such situation is actually frequent in Mediterranean WUI areas.

5.2. Step 1 - fire source characterization

The fire characterization was carried out following Option 2, introducing a solid flame model and assigning a fire emissive power. As shown in Fig. 4, it was assumed that the fire generated during the test
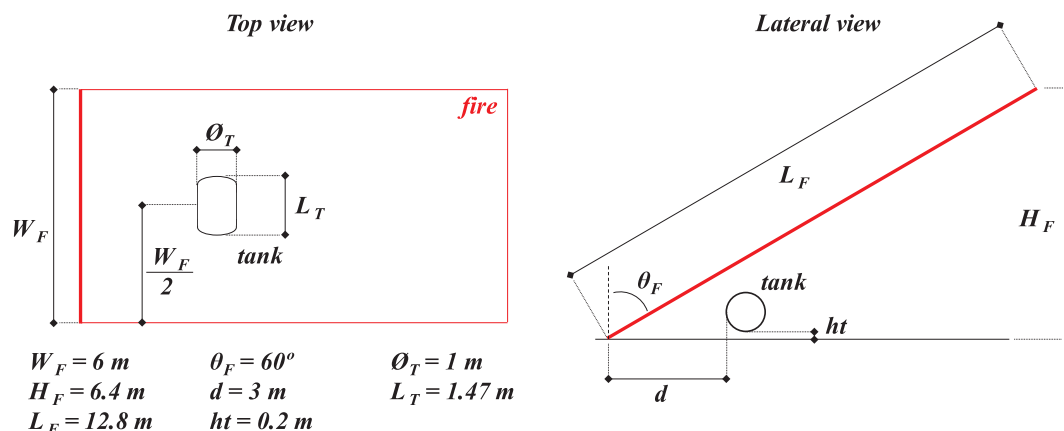

Fig. 4. Geometric characteristics assumed for the fire and relative position with respect to the LPG tank for Scenario 1. The red rectangle represents the fire shape. (For interpretation of the references to colour in this figure legend, the reader is referred to the web version of this article.)

could be approximated to a rectangle with constant shape and dimensions. The rectangle was considered to have an inclination of 60° with respect to simulate the effect of the wind. An emissive power varying according to the transient profile reported in Fig. 5b was assumed (dotted red line).

Based on fire characterization, the incident radiation to the tank wall was calculated. First, the view factors between each of the points lying on the tank wall and the plane representing the fire were calculated following the approach reported in Scarponi et al., 2018b. Fig. 5a shows the results of this calculation. Assuming conservatively a unitary air transmissivity ($\Gamma = 1$ in Eq. (3)), the incident radiation (I_P) at point P on the tank surface was obtained using Eq. (7), where E is the fire emissive power, T_∞ is the temperature of the surrounding (set at 20 °C in this study) and $f_{F \to P}$ is the view factor between the fire and point P.

$$I_P = f_{F \to P} E + (1 - f_{F \to P}) T_\infty{}^4 \qquad (7)$$

Fig. 5b provides an example of how the incident radiation changes considering different points on the surface of the tank wall. It is interesting to note that the values of the incident radiation along the exposed wall (e.g. point A and B in Fig. 5b) are well above the 22 kW/m² suggested as the incident heat flux by the API 2510 standard.

As for T_g and h_g, the convective heat transfer between the tank and the surrounding air was not taken into account. This is a conservative assumption since it eliminates the cooling effect of air.

5.3. Step 2 - tank response simulation

This step consists of the analysis of the tank response by means of CFD modelling. Since in this case study the lay-out is symmetric with respect to the vertical plane (perpendicular to the tank axis) cutting the tank center, only half of the tank was considered in order to save computational time (see Fig. 6a). The problem domain (the tank solid wall and its internal volume, see Fig. 6b) was discretized using an unstructured grid obtained as a combination of tetrahedrons and hexahedrons with a maximum edge size of 3 cm (2 cm for the cell lying onto the external wall). In order to achieve appropriate resolution in the proximity of the inner wall (see Fig. 6c), where the gradients of temperature and velocity are high, the grid was refined defining an inflation region (25 layers with a volume growth rate of 1.1) with a first layer thickness of 0.2 mm. The resulting number of cells was 533,997.

The tank lading was assumed as pure propane, the material properties of which were defined as a function of temperature according to data reported by Liley et al. (1999). The thermal properties of carbon steel were considered for the tank wall (CEN - European Committee for Standardization, 1998). The boundary conditions along the outer wall

were defined according to the results obtained in Step one. The no-slip condition was assigned to the inner wall. At the beginning of the simulation, the fluid was considered to be motionless, the temperature was set to 20 °C and the pressure at 8.36 bar (corresponding to the saturation of pure propane at 20 °C). A value of 18 bar was considered as the opening pressure of the PRV in both cases.

As for the degree of filling, two different cases where analyzed in order to study its effect on the tank response. In the first case, a 20% of liquid was considered (low filling level case, referred to as S1_20% in the following). In the second, an 80% filling level was considered (high filling level case, referred to as S1_80%).

Two additional cases were analyzed (that will be referred to as S1_20%_ins and S1_80%_ins in the following), in which the tank is covered by 20 mm layer of thermal insulation (vermiculite-cement coating, the physical properties of which were taken from Gomez-Mares et al. (2012)). In the CFD simulation the presence of the insulation layer was defined using the shell conduction option available in the software. This creates virtual layers (in this case 4 layer each of which with a thickness of 5 mm) in which the transient heat conduction equation is solved in all the three spatial directions (see ANSYS inc, 2012 for further details).

In the following, the analysis of the data provided by CFD simulations is carried out focusing on pressurization curves and wall temperature profiles, which are the variables of interest when the tank integrity is of concern. A more detailed and fundamental study of CFD results considering, for instance, the temperature distribution in the liquid and vapor phases, evolution of the velocity field and liquid thermal expansion can be found in literature (D'Aulisa et al., 2014; Scarponi et al., 2019, 2018a, 2018b).

Fig. 7a shows the results obtained for the internal pressure. Regardless the filling degree, the pressure increase in the tanks featuring thermal insulation is negligible (≈ 0.1 and ≈ 0.2 bar with respect to the initial pressure for the S1_20%_ins and the S1_80%_ins respectively). The situation drastically changes when thermal insulation is absent. The pressure rise is faster when the tank is 80% full of liquid. Higher values of pressure are attained in this case, where the PRV opens after about 400 s. Differently, in the S1_20% case the pressure remains well below the PRV set point, reaching a maximum value of 13.1 bar.

This difference is due to the contribution of the boiling liquid at the tank wall. In fact, in the case featuring the lowest filling degree, the shell portion wetted by the liquid is exposed to a quite low incident radiation and nucleate boiling occurs in a very limited part of the domain. On the other hand, when the tank is 80% full of liquid, the surface on which boiling takes place is much more extended, producing a fast increase in the vapor phase mass and speeding up the
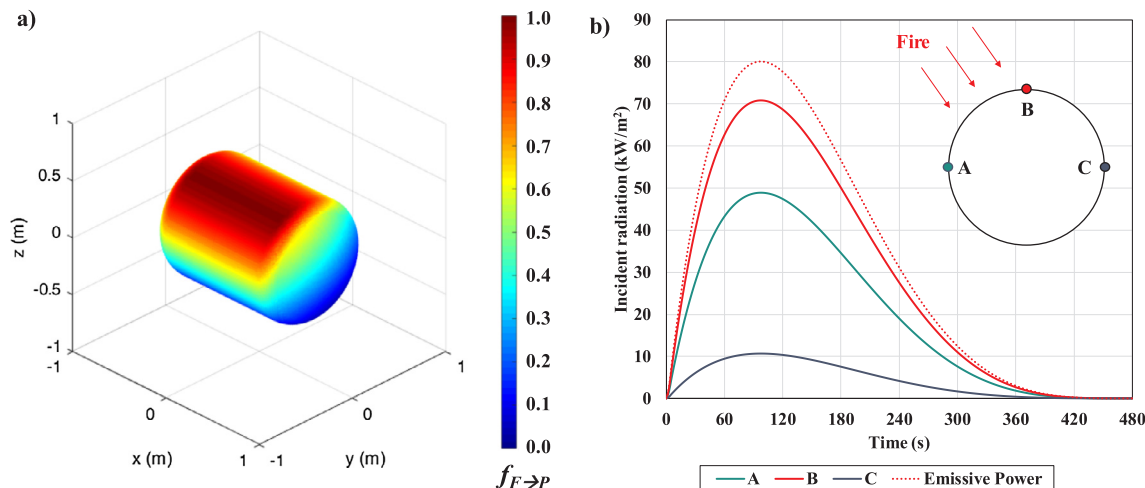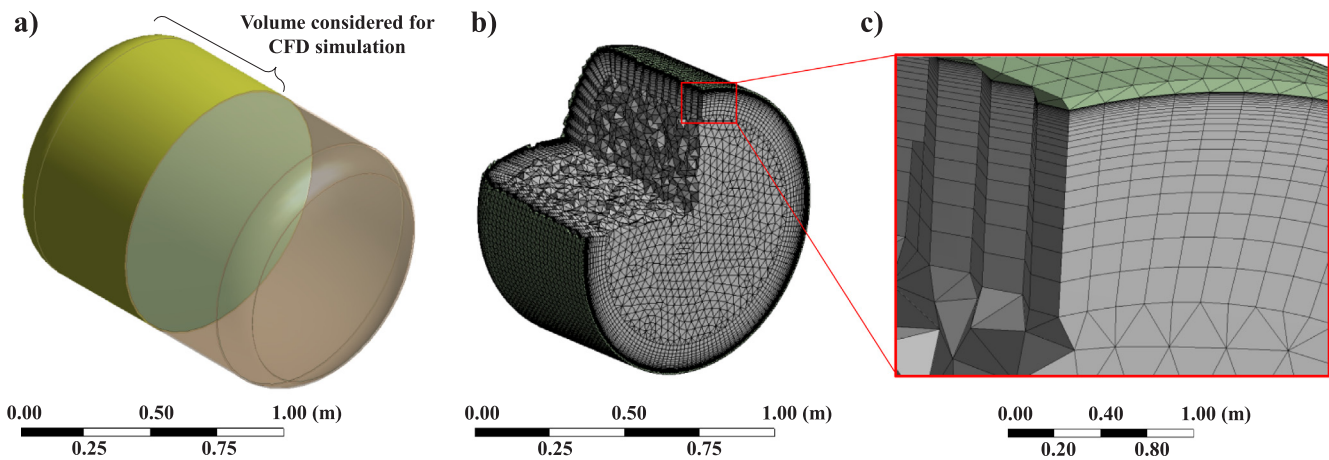
Fig. 5. (a) Contour plot of view factors calculated at tank surface for the lay out shown in Fig. 4; (b) incident radiation vs. time in different positions of the external wall (at the central vertical section) considering an ambient temperature of 20 °C.

Fig. 6. (a) Tank portion considered for the CFD simulation of the tank response; (b) overview of the computational grid; (c) detail showing the increased grid resolution in the near wall region (grey and green cells refer to the fluid and the solid domains respectively). (For interpretation of the references to colour in this figure legend, the reader is referred to the web version of this article.)

pressurization process. It is interesting to notice how the tank keeps pressurizing well beyond the instant of time in which the fire emissive power curve starts decreasing (see Fig. 5, where the curve assumed for the fire emissive power vs. time is reported) and that the pressure inside the tank remains high even when the fire is almost extinguished.

Differently from pressure, Fig. 7b shows that the maximum wall temperature is not influenced by the filling degree in the ranges allowed by national standards (filling degree should be equal or lower than 80 or 85% depending on the country). This is true for all the cases analyzed. In the presence of thermal insulation (cases S1_20%_ins and S1_80%_ins), the temperature increase is very limited ($\approx$ 10 °C with respect to the initial temperature). On the contrary, in both the S1_20% and the S1_80% cases, the peak wall temperature exceeds 400 °C and remains above this threshold for several minutes. Analyzing the temperature distribution over the external wall, it evident that the region suffering mechanical weakening due to the high temperature is quite extended in both cases. This is clearly visible in Fig. 8a and b (data shown refer to S1_20% and S1_80% cases only, in which thermal insulation is not present), where the area of the wall featuring a temperature higher than 400 °C is highlighted in red (data after 240 s of fire exposure are considered). A similar consideration can be made looking at Fig. 8c and d, showing the temperature profiles at intervals of 120 s along the curve given by the intersection between the tank wall and the symmetry plane perpendicular to the tank axis (for cases S1_20% and S1_80% only). It is well visible how the liquid produces a cooling effect on the steel, limiting the temperature in the portion of the wall in contact with the condensed phase. Such behavior is more pronounced when the filling degree is higher.

5.4. Step 3 – Assessment of tank integrity

Specific indicators were calculated on the basis of the results of step 2, to allow understating the impact of the scenario on the safety of the tank. Fig. 9 shows a comparison of the values calculated for the indicators (see Table 2) obtained for the four cases analyzed.

Focusing on the cases where thermal insulation is not present, the PRVI is equal to 1 for the case featuring the higher filling degree (S1_80%) and 0.73 for the other, suggesting that, even considering the uncertainties in the definition of the fire scenario, the risk of having a jet fire generated by the opening of the PRV is quite low for the latter case. The same applies, regardless the filling level, to the cases in which the tank is protected by thermal insulation.

The WSI indicates that, in both the S1_20% and the S1_80% cases, the maximum extension of the area experiencing this phenomenon is higher than the critical value S_C. The values obtained in the the S1_20% (WSI = 1.04) and the S1_80% cases (WSI = 1.29) both exceed the acceptance criteria (0.9) suggested in the present study. On the other hand, when the tank features thermal insulation (cases S1_20%_ins and S1_80%_ins), the WSI equals zero.

It may be concluded that, if no protection measure is in place, Scenario 1 represents a threat for the tank integrity, regardless of the filling degree. On the contrary, Fig. 9 shows that thermal insulation may provide effective mitigation of the risk of tank failure for the scenario analyzed.
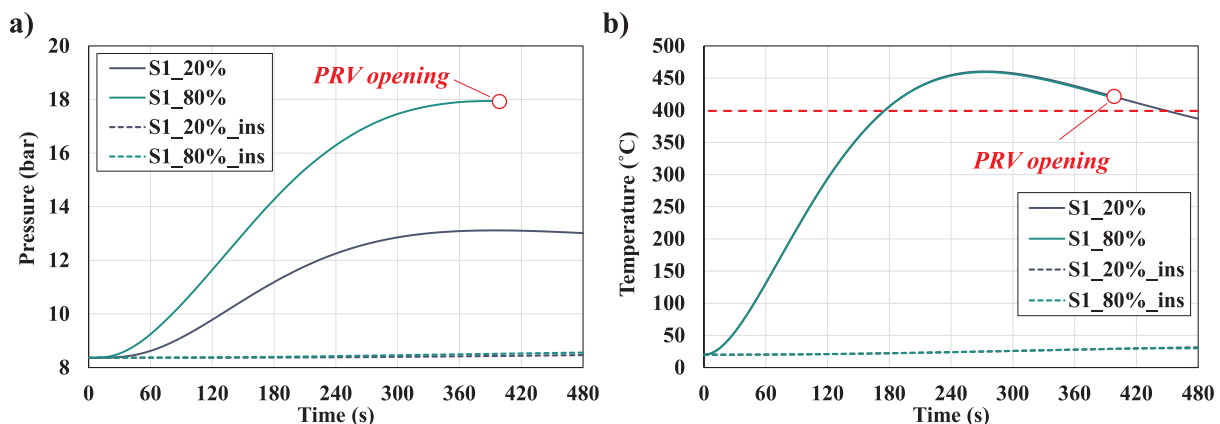
Fig. 7. (a) Pressure vs. time and (b) maximum wall temperature obtained for different filling levels.
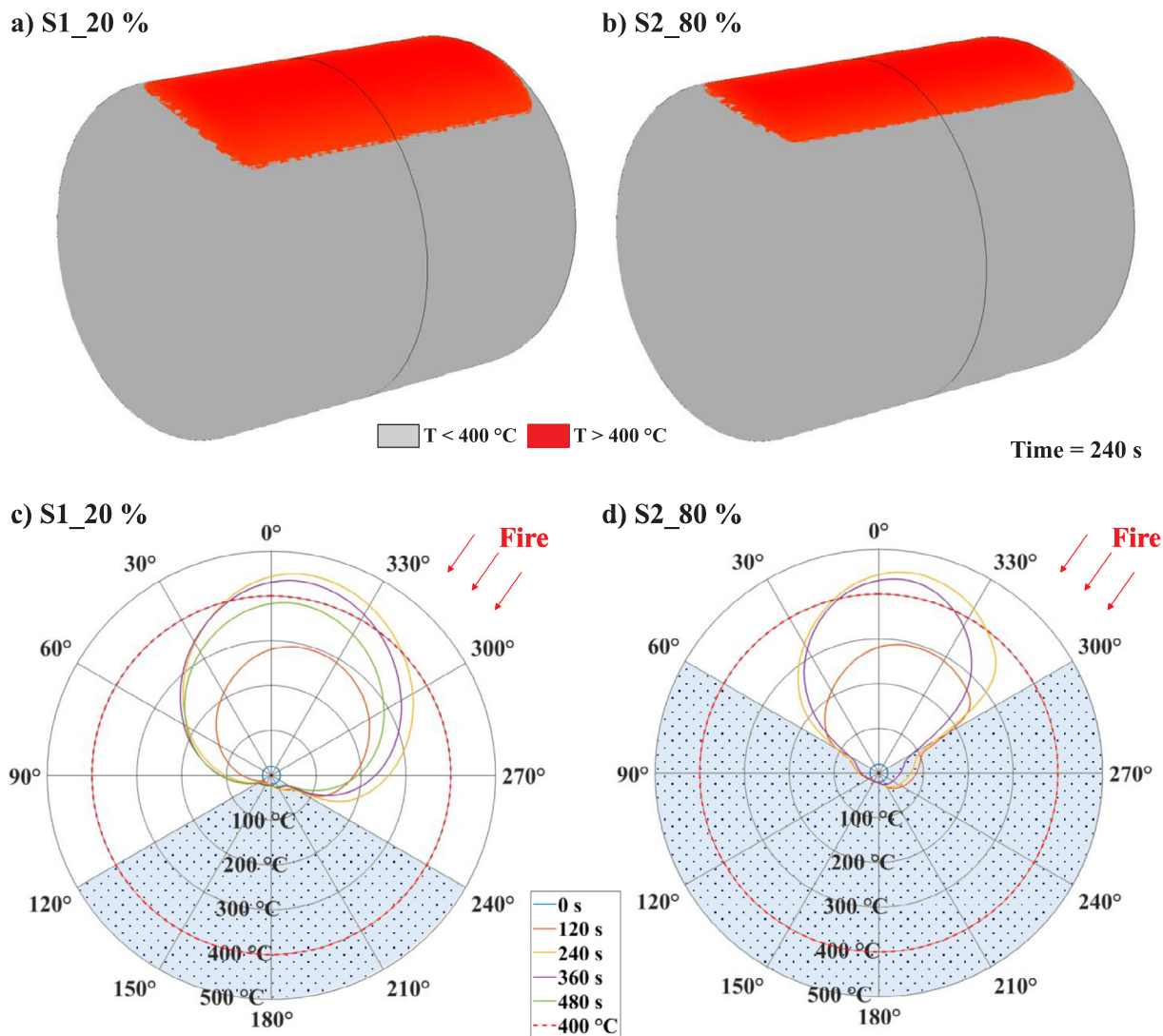
Fig. 8. Region of the external wall with temperatures higher than 400 °C for (a) S1_20%; and (b) S1_80% cases (time = 240 s). External wall temperature profiles at the symmetry plane perpendicular to the tank axis at different intervals of time for (c) S1_20% and the (d) S1_80% cases. The shaded area in the polar plots highlights the portion of the wall wetted by the liquid.

5.5. Scenario 2

A second scenario was analyzed in which the same LPG tank considered for Scenario 1 was exposed to a different reference fire, generated assuming a geometry based on a row of six Douglas fir trees catching fire. The reason at the base of this choice is the availability of literature data describing the burning characteristics of such species. In particular, Mell et al. (2009) reported the results of a set of burning tests carried out on Douglas fir trees in a controlled environment. Fig. 10 shows an overview of geometrical characteristics of Scenario 2, defined on the basis of the data reported by Mell et al. (2009). The trees were assumed 2.05 m high (0.15 m of clear trunk base and 1.90 m of crown), with a conical canopy having a 1.6 m diameter base. The tank was positioned 3 m away from the trees. Two different weather conditions were explored: absence of wind and wind flowing in a direction perpendicular to the tank (see Fig. 10) with the logarithmic speed profile for neutral atmospheric conditions described by Eq. (8):

$$U = A_W \left[ln\left(\frac{z - d_{w0}}{z_0}\right) \right] \tag{8}$$

where U is the wind velocity profile along the vertical coordinate (z), d_{w0} is the height above the ground at which zero wind speed is achieved

as a result of obstacles (d_{w0} = 1.47 m corresponding to 2/3 the height of the ornamental tree), z_0 is the roughness length (0.2 m accounting for the presence of land with trees and bushes) and A_W takes the value of 3.68 to meet u_{10} = 50 km·h^{-1}.

5.6. Step 1 – Fire source characterization

As mentioned above, the analysis of Scenario 2 aims at providing a detailed description of how to apply Option 3.1 and 3.2 for fire source characterization. In both cases, the geometric characteristics of Scenario 2 were reproduced using the FDS6.7.1 software (see Fig. 11a). In the simulations considering the presence of the wind, the wind speed profile calculated according to Eq. (8) was assigned to the boundary colored in blue in Fig. 11a.

In Option 3.1, the trees were modelled as solid cones and the fire was simulated assuming the HRR curve reported in Fig. 11b for the surface of each cone. In Option 3.2, the approach proposed by Mell et al. (2009) was applied (adapting the simulation setup from WFDS to FDS6.7.1). The tree crowns were modelled as distributed solid particles, divided into four size classes according to experimental observations reported by Mell et al. (2009): foliage, roundwood of diameter < 3 mm, roundwood of diameter between 3 and 6 mm and roundwood
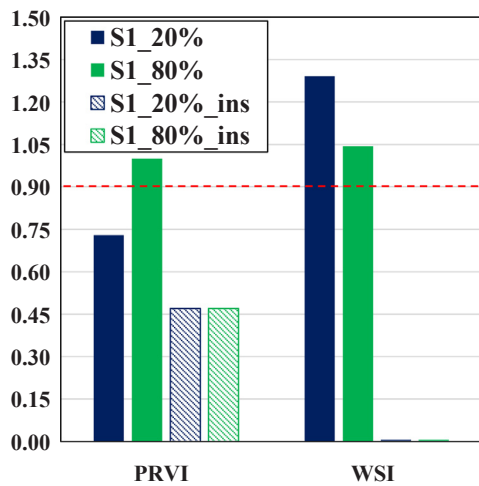
Fig. 9. Comparison of the values of the indicators obtained for the S1_20% (blue bars), the S1_80% (green bars), the S1_20%_ins (withe bars with blue stripes) and the S1_80%_ins cases (withe bars with green stripes). (For interpretation of the references to colour in this figure legend, the reader is referred to the web version of this article.)
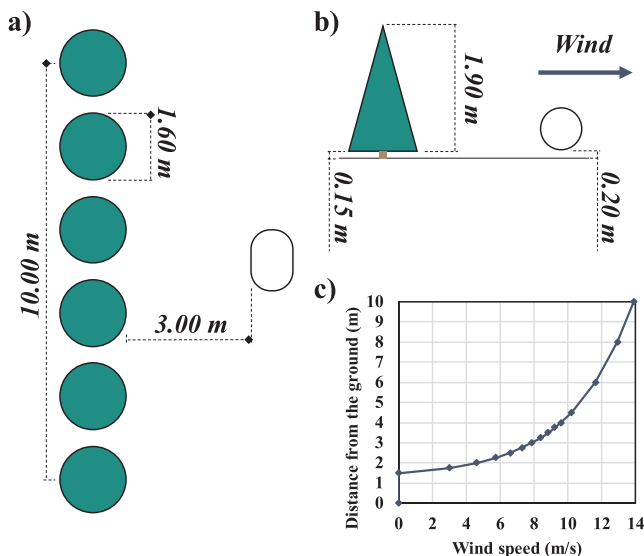
Fig. 10. Lay out (a) and b) lateral view of the trees and of the LPG tank in Scenario 2. Wind speed profile (c) considered for the FDS simulation in windy conditions.

with a diameter between 6 and 10 mm. The total mass burned was assumed of 3.9 kg (dry mass). For all vegetation types, the following parameters were assumed: moisture on a dry weight basis of 14%, dry and wet bulk densities of 2.98 kg/m^3 and 3.4 kg/m^3 respectively.

Given a heat source (simulated introducing a ring shaped hot spot at the base of each tree, which induced a buoyant hot flow), the particles temperature increases and the moisture is removed. Then, the pyrolysis starts and fuel vapors are generated. Finally, the remaining char undergoes an oxidation process. For the sake of brevity, equations describing the pyrolysis process as well as other details on the simulation setup are not reported here. The reader is referenced to the paper of Mell and co-workers (2009) for the full details on the simulation approach.

Fig. 12 reports a series of snapshots showing the characteristics of the fire (after 10 s of simulation) as obtained following Option 3.1 and 3.2.

In calm conditions (Fig. 12a and b) the two modelling approaches show quite similar results, with the most complex one (Option 3.2)

producing a slightly higher flame. On the other hand, when the presence of wind is taken into account (Fig. 12c and d), the change in the flame shape is more evident. This is due to the fact that in Option 3.1 the trees behave as solid obstacles that the wind cannot cross. On the other hand, when particles are used to model the trees, air can flow through the crowns. In both the windy cases, the flame is remarkably tilted towards the tank. However, with the wind speed considered in the simulations, impingement conditions are never reached. It shall be noted that this does not exclude that a stronger wind may cause the flame to be in contact with the tank, increasing the resulting heat load.

The differences (and similarities) in the fire characteristics observed in Fig. 12 are reflected on the heat load to which the tank is exposed. This is visible in Fig. 13a and b comparing the distribution of the incident radiation onto the tank side facing the fire (after 10 s of simulation) obtained in each case considered in Fig. 12. In calm conditions, Options 3.1 and 3.2 produce very similar results, whereas the difference in the incident radiation maps is quite pronounced when wind is blowing. This can also be observed in Fig. 13c, reporting the incident radiation vs time curves at the center of the tank side facing the fire (highlighted with a red cross in Fig. 13c). It is interesting to note how, when Option 3.1 is considered, the difference in the incident radiation between calm and windy conditions are far lower than the one obtained following Option 3.2. In all the four cases, the incident radiation is always lower than 22 kW/m^2. Therefore, according to the API 2510, Scenario 2 would not represent a threat for tank integrity.

5.7. Step 2 – Tank response simulation

The tank response step was carried out using the same setup and computational grid considered for the simulation of Scenario 1. The filling degree was set to 80%. A total of four cases were considered. Two of them, labelled as S2_3.1_C and S2_3.1_W, refer to the scenarios in which the boundary condition was defined according to the spatial and temporal distributions of I, h_g and T_g obtained using Option 3.1, for calm and windy conditions respectively. In the others (S2_3.2_C and S2_3.2_W), the output generated by Option 3.2 was considered.

Fig. 14a shows that, in all cases, the pressure increase in the tank is very limited. The maximum pressure (8.5 bar) is obtained for the S1_3.2_W case and is only 0.14 bar higher than the initial pressure. The curves describing the maximum wall temperature in the two cases (Fig. 14b) show a limited temperature increase: about 11 °C for the S2_3.2_W case, 7 °C for the S2_3.2_C case and 5 °C in the remaining cases.

5.8. Step 3 – Assessment of tank integrity

The results reported in Fig. 14 show that, regardless the presence of wind, Scenario 2 produces negligible effects in terms of pressure increase and temperature rise. This is reflected by the values of the KPIs calculated in Step 3 of the methodology. The PRVI indicator results 0.468, 0.469, 0.468 and 0.472 for the S2_3.1_C, S2_3.2_C, S2_3.1_W and S2_3.2_W cases respectively, whereas the WSI is always equal to zero. Thus, it is possible to conclude that this scenario does not represent a threat for the tank integrity. The results confirm the assumption made after comparing the values of incident radiation in Fig. 13 with the threshold value of 22 kW/m^2 suggested by the API 2510.

5.9. Summary of case study results

The analysis of the case studies presented above provides an example of the application of the three steps of the methodology defined in the present work and summarized in Fig. 3. The first scenario considered consists of a fire from a neighboring fuel bed burning (13 m long by 6 m wide) of *Pinus halepensis* slash. In the second one, the tank was exposed to a burning hedgerow of 6 Douglas fir trees. In both cases, the target was 1 m^3 LPG tank placed at 3 m from the fire. The
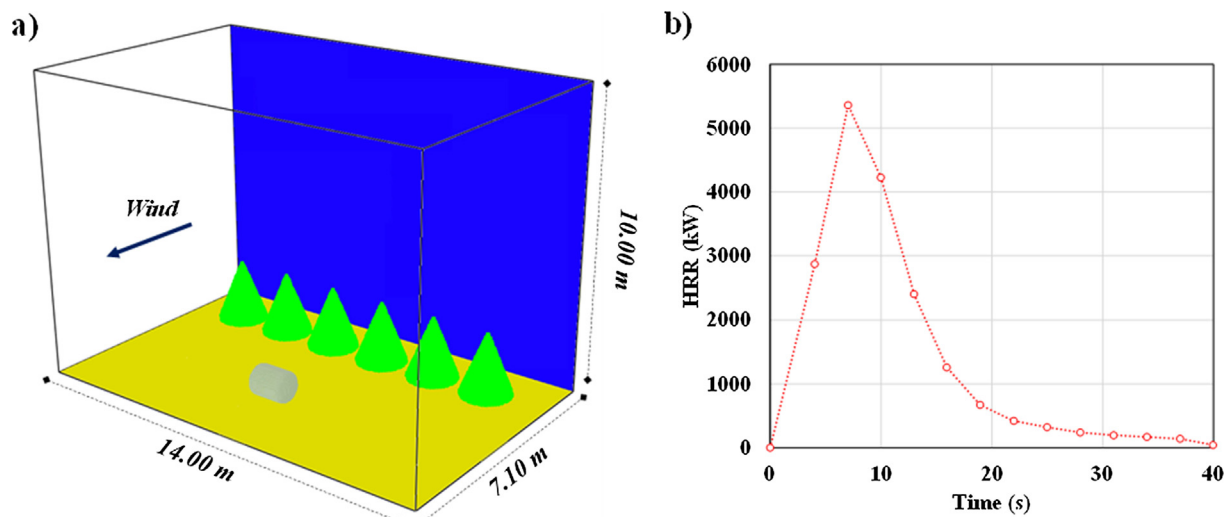
Fig. 11. (a) Computational domain considered for simulation of Scenario 2 using FDS; (b) HRR curve for each of the Douglas fir trees in Scenario 2 obtained from Mell et al. (2009).

assessment of the fire impact on the tank, carried out evaluating the two indicators presented in Step 3, highlighted how Scenario 2 produces negligible effects from the safety point of view, regardless the presence of wind. On the other hand, it was demonstrated that in absence of thermal insulation, Scenario 1 represents a threat for the tank integrity due to the high wall temperatures induced by the fire. Furthermore, it was shown that for high filling degrees (80%), the exposure to the first fire scenario leads to the PRV opening. As mentioned in Section 4.3, this shall be considered as an unwanted event since the jet fire resulting from the ignition of the fluid released by the valve increases the heat load to the tank and may contribute to worsen the consequences of the fire, creating the potential for an escalation of consequences. Finally, it was demonstrated that the presence of thermal insulation may effectively mitigate the effect of the fire on the tank, reducing the risk of failure (and PRV opening).

It is important to remark that the lay out of the tank and the position of the burning vegetation considered in both the fire scenarios analyzed are compatible with the requirements of regulations adopted in Portugal, Spain and UK. Therefore, the results obtained raise some concern about the adequacy of safety distances indicated in the regulations of several European countries.

6. Discussion

The methodology presented in this study provides a tool to assess whether the exposure of a LPG domestic tank to a given fire scenario can be deemed safe.

Characteristics of fire scenarios that may be triggered by a WUI fire

in the proximity of a LPG domestic vessel can vary considerably. They depend, among other factors, on the weather conditions, the type of fuel involved and the mutual position of the tank and the burning material. This makes the determination of the heat load to the tank quite challenging. For this reason, the first step of the proposed methodology presents multiple options to carry out this task. This ensures high flexibility in the variety of fire scenarios that can be analyzed, also according with the degree of detail required by the user and the availability of data.

The limitations of step 1 are a direct consequence of the inherent limitations of the models used in the different options proposed. Option 1, where actually no model is considered, can only be used when the fire load is prescribed. Prescribed fire conditions are usually representative of very simple situations (e.g. full engulfment) and do not allow to capture the complex characteristics of fires scenario at the WUI.

Option 2 is based on the solid flame model, allowing to take into consideration the geometric features of the scenario. The main limitation of this approach is that it cannot be used to simulate fire impingement. Furthermore, it requires the knowledge (or the estimation via simple empirical expressions) of the emissive power and the shape of the flame.

Using Option 3.1 makes possible to simulate fire impingement. Furthermore, flame shape and emissive power are not required as input of the model. However, the user must specify the fire HRR curve. This limits the use of Option 3.1 to the cases for which such parameter is available from experimental data.

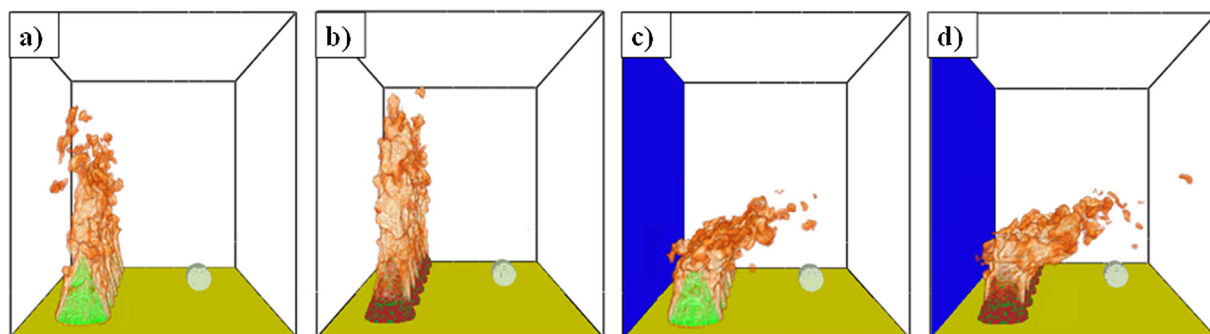Option 3.2 represents the most advanced way of simulating the fire

Fig. 12. Characteristics of the fire in calm (a and b) and windy (c and d) conditions obtained from the fire simulator following Option 3.1 (a and c) Option 3.2 (b and d) after 10 s of simulation.
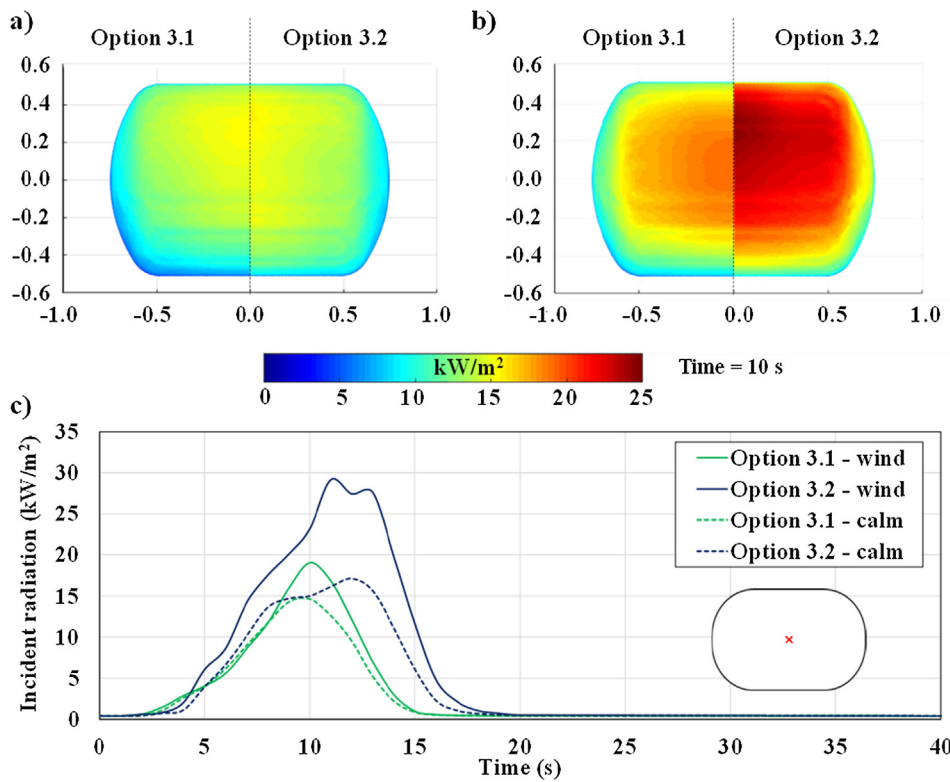
Fig. 13. (a) Distribution of the incident radiation onto the tank side facing the fire (after 10 s of simulation) obtained following Option 3.1 and 3.2 in calm (a) and windy (b) conditions; incident radiation as a function of time at the center of the tank side facing the fire (red cross on tank shell). (For interpretation of the references to colour in this figure legend, the reader is referred to the web version of this article.)

scenario, since the heat released from the fire is not predetermined, but modelled based on specific local conditions. The shortcoming of this approach is that it requires a considerable amount of inputs, such as the composition of the fuel and the parameters characterizing the combustion reactions.

Finally, it should be noted that both Option 3.1 and Option 3.2 are subjected to the inherent limitations of the fire modelling software used in the analysis. For FDS6.7.1, these are reported in the software technical guide (McGrattan et al., 2016).

Being Options 3.1 and 3.2 the ones ensuring the best accuracy among all the options proposed, they should be preferred to carry out the fire characterization step whenever data availability allows their use. Moreover, these are the only options that allow properly considering flame impingement.

The assessment of the tank integrity is the most critical step of the present methodology. Concerning the risk of tank failure, determining whether the tank would rupture under specific fire conditions requires a detailed stress analysis based on full geometrical and mechanical details

of the tank, which is out of the scope of the present study. Instead, an indicator based on the extension of the tank wall surface area suffering mechanical weakening was proposed. This provides an approach to assess whether the tank integrity is under threat. However, this represent a strong simplification if the complex phenomena leading to vessel failure are considered (Manu et al., 2009).

7. Conclusions

Managing Wildland-Urban-Interface (WUI) fires is a challenging task due to the inherent complexity of the WUI environment. To ensure the success of strategies for the protection of population and structures, safety measures have to be implemented at different scales (landscape, community and homeowner). The present study is focused on the homeowner scale and deals with the threat related to the presence of LPG domestic tanks in a WUI fire scenario. Recent accidents have demonstrated that the risk associated with this type of installations is far from negligible, but is often disregarded by residents. The survey of
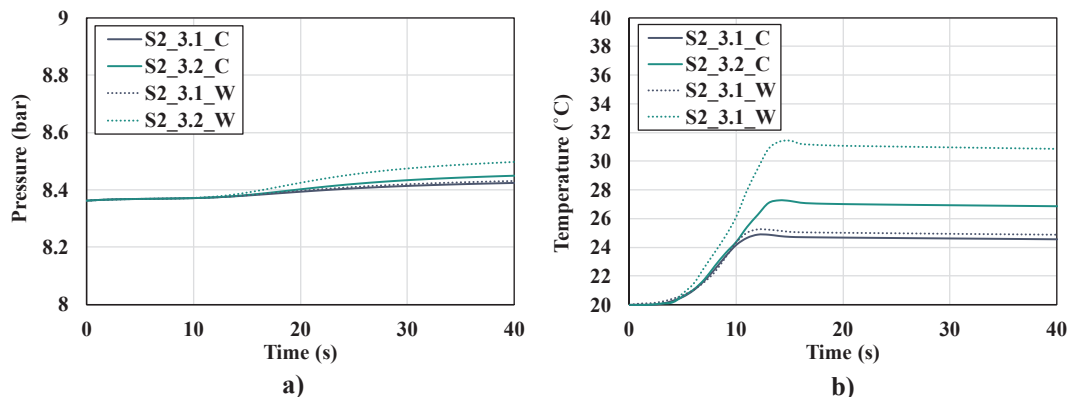

Fig. 14. (a) Pressure curves and (b) maximum wall temperature obtained for the S2_3.1_C (blue solid line), the S2_3.2_C (green solid line), S2_3.1_W (blue dotted line) and the S2_3.2_C (green dotted line) cases. (For interpretation of the references to colour in this figure legend, the reader is referred to the web version of this article.)

regulations detailed in the present study provides evidence of a lack of harmonization throughout European countries. Moreover, important gaps have been highlighted in specific provisions, particularly those referred to the presence of fuels near domestic LPG tanks. Furthermore, there is no general agreement in the definition of safety distances. A 3-step methodology was developed to assess if the integrity of a domestic LPG tank exposed to WUI fire scenarios may be affected. This allows overcoming the limitations of most common wildfire spread models, that are not able to capture specific characteristics of wildfire behavior at the WUI and that, therefore, cannot be used to assess the risk of fire impact of targets in peculiar scenarios as those analyzed in the present study. The results obtained from the application of the methodology to a set of case studies rise some concern about the appropriateness of distances prescribed in the regulations of several European countries. Thus, future work will be devoted to the identification and the analysis of typical WUI fire scenarios involving LPG tanks, in order to carry out a critical assessment of current prescriptions related to this kind of installation and highlight possible gaps in safety regulations. Outcomes from this modelling approach are envisaged to be the basis of scientific-based recommendations for future policy improvements and may contribute to a more sound and harmonized definition of safety distances for LPG domestic tank at the WUI.

Acknowledgments

References

Abbasi, T., Abbasi, S.a., 2007. The boiling liquid expanding vapour explosion (BLEVE): mechanism, consequence assessment, management. J. Hazard. Mater. 141, 489–519. https://doi.org/10.1016/j.jhazmat.2006.09.056.

American Petroleum Institute, 2001. Design and Construction of LPG Installations, API STANDARD 2510 eighth edition.

Anderson, W., Pastor, E., Butler, B., Catchpole, E., Dupuy, J.-L., Fernandes, P., Guijarro, M., Mendes-Lopes, J.-M., Ventura, J., 2006. Evaluating models to estimate flame characteristics for free-burning fires using laboratory and field data. For. Ecol. Manage. https://doi.org/10.1016/j.foreco.2006.08.113.

Asociación Española de Normalización y Certificación, 2008. Instalaciones de almacenamiento de gases licuados del petróleo (GLP) en depósitos fijos para su consumo en instalaciones receptoras. UNE 60250:2008. Madrid.

Aydemir, N.U., Magapu, V.K., Sousa, A.C.M., Venart, J.E.S., 1988. Thermal response analysis of LPG tanks exposed to fire. J. Hazard. Mater. 20, 239–262. https://doi.org/10.1016/0304-3894(88)87015-8.

Babrauskas, V., Peacock, D.R., 1992. Heat release rate: the single most important parameter in fire hazard. Fire Saf. J. 18, 255–272.

Beatty, K.O., 2004. Thermal radiation heat transfer, second edition, Robert Siege1 and John R. Howell, hemisphere publishing corporation, 862 pages,$32.00. A solutions manual is available. 1981. AIChE J. https://doi.org/10.1002/aic.690270426.

Beynon, G.V., Cowley, L.T., Small, L.M., Williams, I., 1988. Fire engulfment of LPG tanks: HEATUP, a predictive model. J. Hazard. Mater. 20, 227–238. https://doi.org/10.1016/0304-3894(88)87014-6.

Bi, M.S., Ren, J.J., Zhao, B., Che, W., 2011. Effect of fire engulfment on thermal response of LPG tanks. J. Hazard. Mater. 192, 874–879.

Birk, A., Cunningham, M.H., 1994. The boiling liquid expanding vapour explosion. J. Loss Prev. Process Ind. 7, 474–480.

Birk, A.M., 2006. Fire testing and computer modelling of rail tank-cars engulfed in fires: literature review.

Birk, A.M., 2005. Tank-car thermal protection defect assessment : updated thermal modelling with results of fire testing.

Birk, A.M., 1995. Scale effects with fire exposure of pressure-liquefied gas tanks. J. Loss Prev. Process Ind. 8, 275–290. https://doi.org/10.1016/0950-4230(95)00028-Y.

Birk, A.M., 1988. Modelling the response of tankers exposed to external fire impingement. J. Hazard. Mater. 20, 197–225. https://doi.org/10.1016/0304-3894(88)87013-4.

Birk, A.M., 1983. Development and validation of a mathematical model of a rail tank-car engulfed in fire. Dev. Valid. a Math. Model a Rail Tank-car Engulfed Fire. PhD Thesis. Queen's University, Kingston, Ontario, Canada.

Birk, A.M., Cunningham, M.H., 1996. Liquid temperature stratification and its effect on BLEVEs and their hazards. J. Hazard. Mater. 48, 219–237.

Bray, G.A., 1964. Fire protection of liquefied petroleum gas strorage tanks. IGE J.

CEN - European Committee for Standardization, 1998. EN 10222-1. Steel forgings for pressure purposes. Part 1: General requirements for open die forgings. European Committee for Standardization, Brussels.

Cozzani, V., Antonioni, G., Landucci, G., Tugnoli, A., Bonvicini, S., Spadoni, G., 2014. Quantitative assessment of domino and NaTech scenarios in complex industrial areas. J. Loss Prev. Process Ind. 28, 10–22. https://doi.org/10.1016/j.jlp.2013.07.009.

D'Aulisa, A., Tugnoli, A., Cozzani, V., Landucci, G., Birk, A.M., 2014. CFD modeling of LPG vessels under fire exposure conditions. AIChE J. 60, 4292–4305. https://doi.org/10.1002/aic.14599.

Delvosalle, C., Fievez, C., Pipart, A., Debray, B., 2006. ARAMIS project: a comprehensive methodology for the identification of reference accident scenarios in process industries. J. Hazard. Mater. 130, 200–219.

Diario da República, 2002. Decreto-Lei no 246/92 de 30 de Outubro, do Regulamento de Construçao e Explorazao de Postos de Abastecimento de Combustíveis.

Eckert, E.R.G., 2004. Radiative transfer, H. C. Hottel and A. F. Sarofim, McGraw-Hill Book Company, New York, 1967. 52 pages. AIChE J. https://doi.org/10.1002/aic.690150504.

Eisenberg, N.A., Lynch, C.J., Breeding, R.J., 1975. Vulnerability model. A simulation system for assessing damage resulting from marine spills. Final report.

Finney, M., 1994. FARSITE: a fire area simulator for fire managers. Proc. Biswell Symp. 55–56.

Finney, M.A., 2006. An overview of FlamMap fire modeling capabilities. Fuels Manag. to Meas. Success Conf. Proc. 213–220.

Gazzetta Ufficiale Della Repubblica Italiana, 2004. Decreto Legislativo del 14 Maggio 2004, published in GUSG n. 120 del 24 Maggio.

Germany, W., Dancer, D., Sallet, D.W., 1990. Pressure and temperature response of liquefied gases in containers and pressure vessels which are subjected to accidental heat input 25, 3–18. 10.1016/0304-3894(90)85066-C.

Gomez-Mares, M., Tugnoli, A., Landucci, G., Cozzani, V., 2012. Performance assessment of passive fire protection materials. Ind. Eng. Chem. Res. 51, 7679–7689. https://doi.org/10.1021/ie201867v.

Gong, Y.W., Lin, W.S., Gu, A.Z., Lu, X.S., 2004. A simplified model to predict the thermal response of PLG and its influence on BLEVE. J. Hazard. Mater. 108, 21–26. https://doi.org/10.1016/j.jhazmat.2004.01.012.

Graves, K.W., 1973. Development of a Computer Model for Modeling the Heat Effects on a Tank Car. US Department of Transportation, Federal Railroad Administration, Washington DC.

Hadjisophocleous, G.V., Sousa, A.C.M., Venart, J.E.S., 1990. A study of the effect of the tank diameter on the thermal stratification in LPG tanks subjected to fire engulfment. J. Hazard. Mater. 25, 19–31.

Health and Safety Executive (Hse), 2016. Safe use of liquefied petroleum gas (LPG) at small commercial and industrial bulk installations 1–16.

Heymes, F., Aprin, L., Ayral, P.A., Slangen, P., Dusserre, G., 2013a. Impact of Wildfires on LPG Tanks. Chem. Eng. Trans. 31, 637–642. https://doi.org/10.3303/CET1331107.

Heymes, F., Aprin, L., Birk, A.M., Slangen, P., Jarry, J.B., François, H., Dusserre, G., 2013b. An experimental study of an LPG tank at low filling level heated by a remote wall fire. J. Loss Prev. Process Ind. 26, 1484–1491.

Heymes, F., Aprin, L., Forestier, S., Slangen, P., Baptiste, J., François, H., Dusserre, G., 2013c. Impact of a distant wildland fire on an LPG tank. Fire Saf. J. 61, 100–107.

Hurley, M.D., Gottuk, J., Hall, K., Harada, C., Kuligowski, E., Puchovsky, M., Torero, J., Watts, J., Wieczorek, C., 2002. SFPE handbook of fire protection engineering (1995). Fire Saf. J. https://doi.org/10.1016/s0379-7112(97)00022-2.

Inc, A., 2012. ANSYS® FLUENT® 14.5 Theory Guide. ANSYS Inc, Cecil Township, PA.

Johnson, M.R., 1998a. Tank Car Thermal Analysis, Volume 1, User's Manual for Analysis Program. Department of Transportation, Federal Railroad Administration, Washington DC.

Johnson, M.R., 1998b. Tank Car Thermal Analysis, Volume 2, Technical Documentation Report for Analysis Program. US Department of Transportation, Federal Railroad Administration, Washington DC.

Journal Officiel République Française, 1979. Arrêté du 30/07/79 relatif aux règles techniques et de sécurité applicables aux stockages fixes d'hydrocarbures liquéfiés non soumis à la législation des installations classées ou des immeubles recevant du public.

Khakzad, N., 2019. Modeling wildfire spread in wildland-industrial interfaces using dynamic Bayesian network. Reliab. Eng. Syst. Saf. https://doi.org/10.1016/j.ress.2019.04.006.

Khakzad, N., Dadashzadeh, M., Reniers, G., 2018. Quantitative assessment of wildfire risk in oil facilities. J. Environ. Manage. 223, 433–443. https://doi.org/10.1016/j.jenvman.2018.06.062.

Krausmann, E., Cozzani, V., Salzano, E., Renni, E., 2011. Industrial accidents triggered by natural hazards: an emerging risk issue. Nat. Hazards Earth Syst. Sci. 11, 921–929. https://doi.org/10.5194/nhess-11-921-2011.

Landucci, G., Gubinelli, G., Antonioni, G., Cozzani, V., 2009. The assessment of the damage probability of storage tanks in domino events triggered by fire. Accid. Anal. Prev. 41, 1206–1215. https://doi.org/10.1016/j.aap.2008.05.006.

Leslie, I.R.M., Birk, A.M., 1991. State of the art review of pressure liquefied gas container failure modes and associated projectile hazards. J. Hazard. Mater. https://doi.org/10.1016/0304-3894(91)87083-E.

Liley, P.E., Thomson, G.H., Friend, D.G., Daubert, T.E., Buck, E., 1999. Physical and chemical data, Section 2. Perry's Chemical Engineers' Handbook. McGraw Hill, New York, NY.

Manu, C.C., Birk, A.M., Kim, I.Y., 2009. Stress rupture predictions of pressure vessels exposed to fully engulfing and local impingement accidental fire heat loads. Eng. Fail. Anal. 16, 1141–1152.

Manzello, S.L., Blanchi, R., Gollner, M.J., Gorham, D., McAllister, S., Pastor, E., Planas, E., Reszka, P., Suzuki, S., 2018. Summary of workshop large outdoor fires and the built environment. Elsevier Ltd. Fire Saf. J. 76–92. https://doi.org/10.1016/j.firesaf.2018.07.002.

Martynenko, O.G., Khramtsov, P.P., 2005. Free-Convective Heat Transfer. Springer-Verlag, Berlin Heidelberg.

Mcdevitt, C.A., 1990. Initiation step of boiling liquid expanding vapor ezplosions. J. Hazard. Mater. 25, 169–180.

McGrattan, K., Hostikka, S., McDermott, R., Floyd, J., Weinschenk, C., Overholt, K., 2016. Fire Dynamics Simulator technical reference guide. NIST Spec. Publ. 1018-1. US Dep. Commer. Natl. Inst. Stand. Technol. Gaithersburg, MD. 1, 175. 10.6028/NIST.SP.1018-1.

Mell, W., Maranghides, A., McDermott, R., Manzello, S.L., 2009. Numerical simulation and experiments of burning douglas fir trees. Combust. Flame 156, 2023–2041. https://doi.org/10.1016/j.combustflame.2009.06.015.

Modest, M.F., 2003. Radiative Heat Transfer. Academic Press, New York, NY.

Moodie, K., 1988a. Experiment and modelling:- an overiview with particular reference to fire engulfment. J. Hazard. Mater. 20, 149–175. https://doi.org/10.1016/0304-3894(88)87011-0.

Moodie, K., 1988b. Experiments and modelling:- An overview with particular reference to fire engulfment. J. Hazard. Mater. 20, 149–175. https://doi.org/10.1016/0304-3894(88)87011-0.

Moodie, K., Billinge, K., Cutler, D.P., 1985. The fire engulfment of LPG storage tanks. IChemE Symp. Ser. No. 93, 87–106.

Murphy, K., Rich, T., Sexton, T., 2007. An Assessment of Fuel Treatment Effects on Fire Behavior, Suppression Effectiveness, and Structure Ignition on the Angora Fire. United States Dep. Agric. 38. http://www.cnpssd.org/fire/angorafireusfsfullreport.pdf.

Naderpour, M., Rizeei, H.M., Khakzad, N., Pradhan, B., 2019. Forest fire induced natech risk assessment: a survey of geospatial technologies. Reliab. Eng. Syst. Saf. https://doi.org/10.1016/j.ress.2019.106558.

Pastor, Elsa, Muñoz, J.A., Caballero, D., Àgueda, A., Dalmau, F., Planas, E., 2019a. Wildland-urban interface fires in Spain: Summary of the policy framework and recommendations for improvement. Fire Technol. https://doi.org/10.1007/s10694-019-00883-z.

Pastor, E., Sebastià, J., Mata, C., Àgueda, A., Valero, M.M., Planas, E., 2019b. Performance analysis of a self-protection system for vehicles in case of WUI fire entrapment. In: Interflam 2019 Conference Proceedings, pp. 1163–1174.

Rehm, R.G., Mell, W.B., 2009. A simple model for wind effects of burning structures and topography on wildland-urban interface surface-fire propagation. Int. J. Wildl. Fire 18, 290–301. https://doi.org/10.1071/WF08087.

Reniers, G., Khakzad, N., Cozzani, V., Khan, F., 2018. The impact of nature on chemical industrial facilities: Dealing with challenges for creating resilient chemical industrial parks. J. Loss Prev. Process Ind. https://doi.org/10.1016/j.jlp.2018.09.010.

Scarponi, G.E., Heymes, F., 2018. CFD study of the behavior of LPG tanks exposed to forest fires 67, pp. 181–186. 10.3303/CET1867031.

Scarponi, G.E., Landucci, G., Birk, A.M., Cozzani, V., 2019. An innovative three-dimensional approach for the simulation of pressure vessels exposed to fire. J. Loss Prev. Process Ind. 61, 160–173. https://doi.org/10.1016/j.jlp.2019.06.008.

Scarponi, G.E., Landucci, G., Birk, A.M., Cozzani, V., 2018a. LPG vessels exposed to fire: Scale effects on pressure build-up. J. Loss Prev. Process Ind. 56, 342–358. https://doi.org/10.1016/J.JLP.2018.09.015.

Scarponi, G.E., Landucci, G., Heymes, F., Cozzani, V., 2018b. Experimental and numerical study of the behavior of LPG tanks exposed to wildland fires. Process Saf. Environ. Prot. 114, 251–270. https://doi.org/10.1016/j.psep.2017.12.013.

Scarponi, G.E., Landucci, G., Tugnoli, A., Cozzani, V., Birk, A.M., 2017. Performance assessment of thermal protection coatings of hazardous material tankers in the presence of defects. Process Saf. Environ. Prot. 105. https://doi.org/10.1016/j.psep.2016.10.009.

Sullivan, A.L., 2009. Wildland surface fire spread modelling, 1990–2007. 1: Physical and quasi-physical models. Int. J. Wildl. Fire 18, 349. https://doi.org/10.1071/wf06143.

Sumathipala, U., Hadjisophocleous, G., Aydemir, N., Yu, C.-M., Sousa, A., Steward, F., Venart, J., 1992. Fire engulfment of pressure-liquefied gas tanks: Experiments and modeling. ASTM Spec. Tech. Publ.

Tugnoli, A., Cozzani, V., Khan, F., Amyotte, P., 2013. Missile Projection Effects, Domino Effects in the Process Industries: Modelling, Prevention and Managing. Elsevier, Amsterdam, The Netherlands.

Tugnoli, A., Moricone, R., Scarponi, G.E., Cozzani, V., 2019. Effective thermal conductivity of fibrous fireproofing materials. Int. J. Therm. Sci. 136, 107–120. https://doi.org/10.1016/j.ijthermalsci.2018.09.035.

Uijt de Haag, P., Ale, B., 1999. Guidelines for Quantitative Risk Assessment: Purple Book. Directorate-General for Social Affairs and Employment.

Venart, J.E.S., 2000. Boiling liquid expanding vapor explosions (BLEVE); possible failure mechanisms and their consequences. IChemE Symp. Ser. No. 147 121–137.

Yoon, K.T., Birk, A.M., 2004. Computational fluid dynamics analysis of local heating of propane tanks.

Yu, C.M., Aydemir, N.U., Venart, J.E.S., 1992. Transient free convection and thermal stratification in uniformly-heated partially-filled horizontal cylindrical and spherical vessels. J. Therm. Sci. 1, 114–122.

ΦΕΚ 477/B/1-7-93, 1993. ΟΙ ΥΠΟΥΡΓΟΙ ΔΗΜΟΣΙΑΣ ΤΑΞΗΣ ΚΑΙ ΒΙΟΜΗΧΑΝΙΑΣ, ΕΝΕΡΓΕΙΑΣ ΚΑΙ ΤΕΧΝΟΛΟΓΙΑΣ.